

DOI: 10.1070/QEL16057

Generation of quantum-electrodynamic cascades in oblique collisions of ultrarelativistic electrons with an intense laser field

A.A. Mironov, A.M. Fedotov, N.B. Narozhny

Abstract. **Quantum-electrodynamic cascade generation is numerically simulated for the case of the oblique collision of a beam of ultrarelativistic electrons with the field of two counterpropagating, focused, circularly polarised laser pulses. It is shown that although the 'collapse and revival' effect is observed at any value of the collision angle, the multiplicity of the cascade essentially depends on this angle and is maximal in the configuration, when the electron beam hits the focus perpendicularly to the optical axis of the laser pulses.**

Keywords: *quantum-electrodynamic cascade, beam of ultrarelativistic electrons, intense laser radiation.*

1. Introduction

Starting from the first predictions of self-sustained quantum-electrodynamic (QED) cascades arising in the interaction of intense laser radiation with matter [1–3], this phenomenon has been intensely discussed in connection with the planned experiments at the next-generation laser facilities, such as ELI [4] and XCELS [5]. The main attention was focused on the cascades arising when the seed electron is placed into the region of an intense laser field [1–3, 6–9], or when a solid-state target is irradiated by intense laser pulses [10, 11] (see also reviews [12, 13]). According to the estimates [3, 6], for the initiation of self-sustained cascades by means of a seed electron the required intensity of laser radiation should be as large as $\sim 10^{24} - 10^{25}$ W cm^{-2}.

Since the maximal intensity achieved at present under laboratory conditions amounts only to 10^{22} W cm^{-2} [14], it seems important to look for the ways of reducing the threshold intensity for cascade generation. Thus, one can reduce it to $10^{23} - 10^{24}$ W cm^{-2} by using multibeam technology and choosing the special polarisation of laser pulses [15]. The practical implementation of the multibeam experiment faces a number of technical difficulties. The choice of optimal polarisation of the laser pulses was discussed also for simpler experimental schemes, in particular, for the field of two counterpropagating laser pulses [16–18]. As a rule, in all such schemes the possibility of placing seed electrons into the centre of the focal region is explicitly or implicitly assumed [1–3, 6, 15–18]. However, practically it can be impossible because of pushing the electrons off the focus by ponderomotive forces.

The QED cascades arise also in the collisions of ultrarelativistic electrons with the laser field* [20, 21]. In this case, one should distinguish between the two types of cascades. In the cascades of 'shower' type (S-type), the secondary particles appear at the expense of the energy of seed particles. In the self-sustained cascades of 'avalanche' type (A-type), every generation of the secondary particles on average restores its energy due to the acceleration by the field, so that finally the energy for the cascade development is borrowed from the field [22]. In the considered scheme at the first stage the electron beam gives rise to an S-cascade; however, if the energy of the initial particles is exhausted before the end of the laser pulse passage, then the created secondary particles at the second stage launch the A-cascade**. In Ref. [22] we referred such two-stage process to as the effect of 'collapse and revival' of the cascade. Such an injection scheme for the seed particles seems to be sufficiently promising from the point of view of the possible experimental implementation.

In Ref. [22] we supposed that the electron beam is injected along the axis of the counterpropagating focused laser pulses, which is apparently hard to implement practically. In the present work we study the same scenario, but in a more general situation, when the axis of the electron beam is oblique with respect to the axis of the counterpropagating laser pulses (Fig. 1). The main attention is focused on the dependence of the cascade dynamics on the collision angle Θ, the electron beam being described by an ensemble of particles with similar initial parameters.

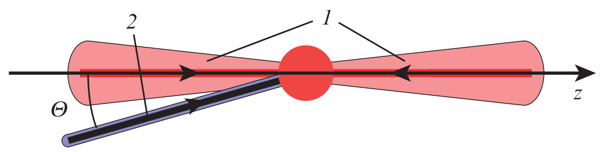

Figure 1. Scheme of cascade initiation in the oblique collision of two counterpropagating circularly polarised focused laser pulses (*1*) and the high-energy electron beam (*2*) incident at the angle Θ.

*Individual events of hard photon emission and creation of electron–positron pairs in the laser field were observed in the E-144 experiment at SLAC [19].

**It seems that actually the A-cascade is launched by the secondary hard gamma-quanta, since the electrons actually cannot penetrate into the focal region because of the strong radiative friction [23].

A.A. Mironov, A.M. Fedotov, N.B. Narozhny National Research Nuclear University 'MEPhI', Kashirskoye sh. 31, 115409 Moscow, Russia; e-mail: am_fedotov@mail.ru

Received 5 February 2016
Kvantovaya Elektronika **46** (4) 305–309 (2016)
Translated by V.L. Derbov

2. Basic approximations

As in earlier papers [3, 6, 22], we consider the cascade dynamics in the external intense laser field using the approximation of a locally constant field. Namely, we suppose that the frequency ω of the laser field with the potential A^ν corresponds to the optical range (for definiteness let us assume $\hbar\omega = 1$ eV), and the peak field strength E_0 is such that the invariant parameter $\xi = e\sqrt{-\langle A^\nu A_\nu \rangle}/mc \simeq eE_0/mc\omega \gg 1$, where the averaging is performed over the field cycle; e and m are the absolute values of charge and mass of the electron. In this case the characteristic length, at which an electron emits a photon, or at which an electron–positron pair is created from a photon, $l_{\rm f} \approx \lambda/\xi \ll \lambda$, will be small compared to the characteristic scale of the field nonuniformity, thus making it possible to use the expressions for the probability of these processes derived for a constant uniform field. Moreover, since in the intense field ($\xi \gg 1$) the particles are ultrarelativistic, it is also possible to assume that locally the particle interacts with the crossed ($\boldsymbol{E} \perp \boldsymbol{H}$, $E = H$) electromagnetic field [3].

The expressions for the probability of the processes of emission and pair creation per unit time in the constant crossed field are known [24, 25]. They are determined by the value of the invariant quantum dynamic parameter $\chi = e\hbar\sqrt{-(F_{\sigma\nu}p^\nu)^2}/m^3c^4$, where $F_{\sigma\nu}$ is the electromagnetic field tensor; and p^ν is the momentum four-vector of the initial particle (electron or photon). In the case when $\chi \gtrsim 1$, the elementary event should be considered within the frameworks of quantum electrodynamics. If $\chi \ll 1$, then the process of emitting photons by the charged particles can be described also within the frameworks of classical electrodynamics, and the probability of pair creation is exponentially suppressed: $W_{\rm cr} \propto \exp(-8/3\chi)$ [24]. The cascade formation is possible for such parameters of the laser pulse that $\chi \gtrsim 1$ for the dominant fraction of the particles and photons, that is why we will consider all elementary processes within the framework of quantum electrodynamics.

In the present paper we consider the initiation of cascades in the vicinity of the threshold intensity of the laser field [3] $I \sim 10^{24}$ W cm^{-2} $\ll I_{\rm s}$, where $I_{\rm s} \approx 5\times10^{29}$ W cm^{-2} is the intensity, corresponding to the so called critical field strength $E_{\rm s} = m^2c^3/eh$. Since the particles in the cascade are ultrarelativistic, this allows one to consider the motion of electrons between the photon emission events quasi-classically with good accuracy [26]. Therefore, we assume that between the emission events the electrons and positrons move with the velocity v along classical trajectories, determined by the classical equation of motion $\dot{\boldsymbol{p}} = -e(\boldsymbol{E} + \boldsymbol{v}\times\boldsymbol{H}/c)$. The photons are localised and move rectilinearly with the speed of light. Note that in the equations of motion one should not specially allow for the radiative friction force, since it is automatically taken into account by the recoil in the course of photon emission [6].

3. Monte Carlo modelling of the cascades

To calculate the QED cascade dynamics in the laser field of arbitrary configuration we elaborated the computer code based on the Monte Carlo method. The basic assumptions of the algorithms are as follows. All particles (electrons, positrons and photons) are pointlike and move along classical trajectories in the laser field. These trajectories are determined by numerical integration of the classical equations of motion. The moments of time, at which the events of emission or pair creation occur, are determined using the Monte Carlo method [7, 27].

When a new photon, electron, or positron is born*, the value of the optical path length $n_{\rm f} = -\ln\eta$ till the first decay is specified for it [η being a random number uniformly distributed in the interval (0, 1)], and the 'current' value of the optical path length is initialised ($n = 0$). Then for this particle the equations of motion are solved on a certain temporal grid; at each time step t_i the 'current' optical path length n is increased by $W(t_i)\Delta t$. Here $W(t_i)$ is the total probability of the corresponding decay (emission of a photon by an electron or electron–positron pair birth) per unit time, determined by the field taken on the particle trajectory at the moment t_i, and Δt is the step of the temporal grid. The moment of the quantum event (photon emission or pair creation) $t_{\rm f}$ is found from the equation $n(t_{\rm f}) = n_{\rm f}$. The energy of the photon (electron) in the process of emission (pair creation by a photon) is determined using the known distribution of the probability density over the energies [6, 24, 25] using the rejection sampling. Within the frameworks of ultrarelativistic particle approximation, we assume that the secondary particles are emitted forward. The energy of the second emitted particle (electron or positron) is found from the conservation law for the dynamic quantum parameter χ (see, e.g., [6]). Note that in contrast to Ref. [6], the considered algorithm completely allows for the recoil in the emission of any photons, including the soft ones.

It is worth noting that the choice of the method for solving the classical equations of motion for relativistic particles is essential, since due to the exponential dependence of the number of particles on time, even minor errors in the calculation of trajectories may produce essential changes in the simulation results. In the program elaborated by us the algorithm of Ref. [28] is used. The program was tested and proved to reproduce the earlier published results [6, 29] (see Appendix).

4. Cascade dynamics in the collision of an electron beam with the field of two counterpropagating laser pulses

By means of the developed programme, we simulated the QED cascades generated in the oblique collision of a monoenergetic beam of electrons in the xz plane with the field of two counterpropagating circularly polarised focused laser pulses (see Fig. 1). The aim of the simulation was to study the dependence of the cascade parameters on the angle Θ between the electron beam and the optical axis z of the laser pulses. The parameters of the electron beam and laser pulses coincide with those of Ref. [22], where the same process was considered at $\Theta = 0$. These parameters allow the observation of the collapse and revival of the cascades. Their values are as follows: the amplitude of the total field of the two laser pulses $E_0 = 3.2\times10^{-3}E_{\rm s}$ (which corresponds to the peak intensity of each pulse $I \sim 10^{24}$ W cm^{-2}), the duration of laser pulses $\tau_{\rm L} = 10$ fs, and the initial energy of the electron beam $\varepsilon_0 = 3$ GeV. To describe the field in the focused circularly polarised laser pulse we used the model, proposed in Ref. [30], with the focusing parameter $\Delta = \lambda/2\pi R = 0.1$, where R is the radius of the focal spot. The simulation started at the time moment $t = -0.6\tau_{\rm L}$; at this moment the laser pulses and the electron beam were prepared so that in the absence of interaction they would

*The electrons and positrons after emitting a photon are also treated as newborn.

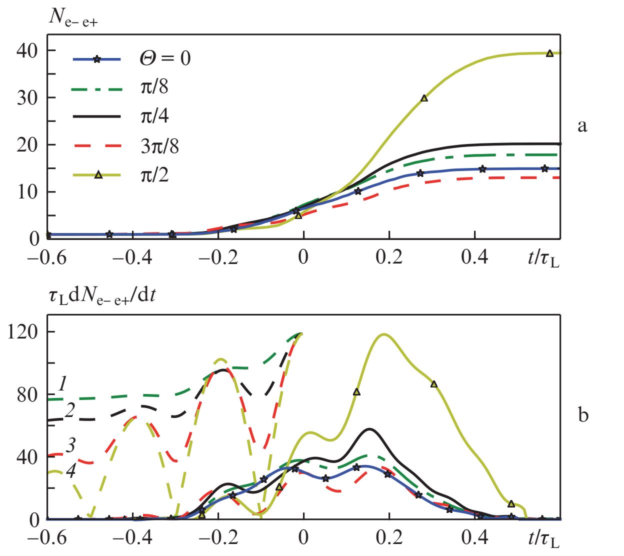

Figure 2. Number of electron–positron pairs N_{e-e+} in the cascade normalised to the number of electrons in the incident electron beam (a) and the rate of its growth dN_{e-e+}/dt (b) versus the normalised time for different tilt angles of the electron beam Θ. The thin dashed lines correspond to the amplitudes of the transverse field (in rel. units) on the electron beam trajectory at $t < 0$ for the cases $\Theta = \pi/8$ (*1*), $\pi/4$ (*2*), $3\pi/8$ (*3*) and $\pi/2$ (*4*).

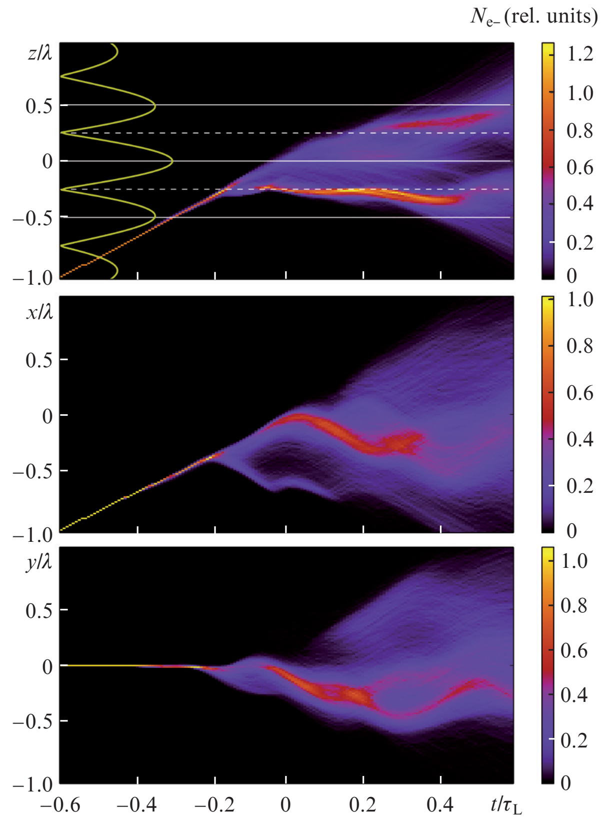

Figure 3. Evolution of the spatial distribution of electrons along the coordinate axes. At the left side of the top picture the plot shows the absolute value of the electric field strength (in rel. units) at the optical axis versus the coordinate z at the moment of time $t = 0$.

meet at the origin of coordinates at $t = 0$. The results of the simulation for different values of Θ are presented in Figs 2–6.

For small angles Θ the growth rate for the number of pairs in the cascade is qualitatively unchanged as compared to the case $\Theta = 0$, described in Ref. [22]. Thus, for $\Theta = \pi/8$ the corresponding curve in Fig. 2b still has a characteristic double-hump structure, in which the first peak corresponds to the cascade of S-type and the second one to the cascade of A-type. However, for further growth of the angle Θ the dependence of the pair production rate in the cascade is somewhat complicated by the fact that at $t < 0$ (when the S-type cascade still dominates) one can observe the appearance of new peaks. This happens because the field component, transverse to the obliquely incident electron beam, $E_\perp(t, \mathbf{r}(t)) \sim \sqrt{E_x^2(t, \mathbf{r}(t))\cos^2\Theta + E_y^2(t, \mathbf{r}(t))}$, which determines the dynamic quantum parameter value for the beam electrons (and, therefore, the probabilities of generating secondary particles), pulsates with time [see curves (*1*–*4*) in Fig. 2]. One can see that the intervals of increase and decrease in the derivative $dN_{e-e+}(t)/dt$ correspond to the increase and decrease in the transverse field amplitude.

Consider in more detail the cascade dynamics by the example of the case $\Theta = \pi/4$. Figure 3 presents the evolution of electron distribution along the coordinate axes. One can see how at the first stage the electron beam moves rectilinearly, entering the region of a strong field. The mean energy of the electrons monotonically decreases, the parameter χ oscillates, taking sufficiently large values (Fig. 4), and the number of particles grows (see Fig. 2), i.e., the S-type cascade takes place. Then to the moment of time $t \approx -0.2\tau_L$, the beam loses almost all its initial energy and the S-type cascade begins to 'collapse'. Part of electrons declines from the initially rectilinear trajectory of motion. Finally, at $t \approx -0.1\tau_L$ the secondary particles reach the region of the central antinode of the electric field. At this moment a new burst of the electron–positron pair creation occurs, most particles starting to move in the polarisation plane xy, i.e., the acceleration mechanism is switched on. During this stage the values of the parameter χ and the energy of the particles take the values close to those predicted by the qualitative theory of self-sustained cascades [3, 6],

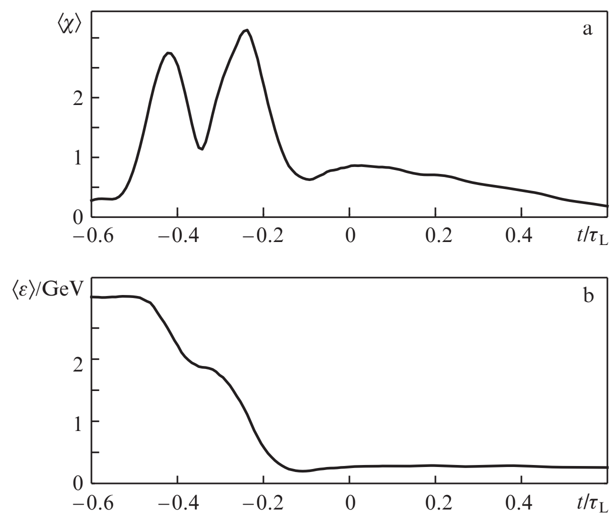

Figure 4. Time dependences of the mean value of the dynamic quantum parameter (a) and the mean value of energy (b) of the electrons in the cascade for $\Theta = \pi/4$.

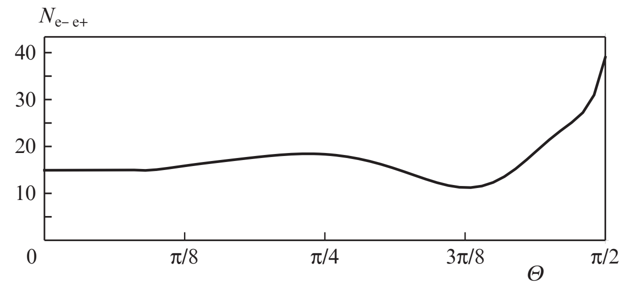

Figure 5. Total number of pairs created in the cascade, normalised to the number of electrons in the intial beam, versus the angle of incidence of the electron beam Θ.

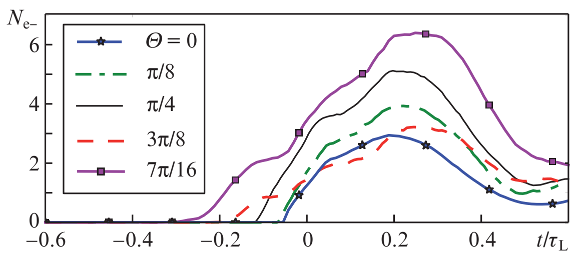

Figure 6. Dependence of the number of electrons (normalised to the number of electrons in the initial beam) in the region of the central field antinode ($|z| < \lambda/8$) on time at different values of Θ.

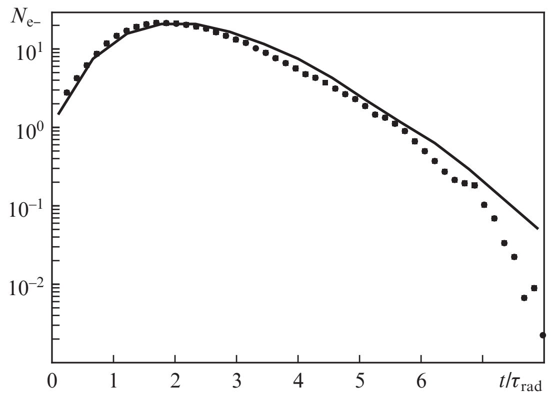

Figure 7. Profile of the cascade initiated by the electron with the energy $\varepsilon_0 = 2\times10^5 mc^2$ in the magnetic field with the strength $H = 0.2E_s$. Solid line shows the results of Ref. [29]; the points show the simulation results.

$$\chi_{est} \simeq \mu^{3/2} \simeq 0.3, \quad \varepsilon_{est} = mc^2\mu^{3/4}\sqrt{\frac{mc^2}{\hbar\omega}} \simeq 0.2 \text{ GeV}, \qquad (1)$$

where $\mu = E_0/\alpha E_s$ is the dimensionless field strength, and α is the fine structure constant. Thus, the first two peaks of the pair creation rate in Fig. 2 corresponds to the S-type cascade, while the last one corresponds to the A-type cascade. This cascade develops until the laser pulses are over. Similar behaviour is observed for other values of the angle Θ.

It is interesting that during the cascade development the electrons and positrons gradually concentrate near the planes $z \approx \pm\lambda/4$ of the electric field nodes (their position is shown by dashed lines at the top in Fig. 3). In these regions, the sedimentation of slow particles from the S-type cascade occurs, and towards these regions the particles are pushed in the course of the A-type cascade development due to the effect of

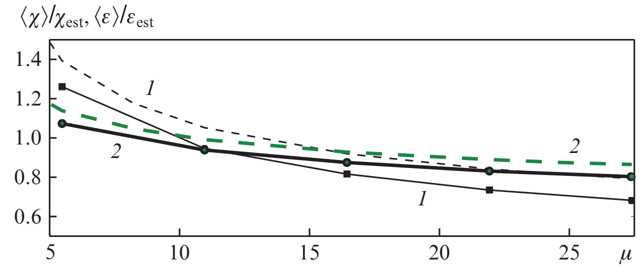

Figure 8. Mean parameters of QED cascades in the uniform rotating electric field $\langle\chi\rangle/\chi_{est}$ (*1*) and $\langle\varepsilon\rangle/\varepsilon_{est}$ (*2*). Solid lines are the result of simulation, dashed lines are the results of Ref. [6].

the 'normal' radiative trapping [31]. The dependence of the total number N_{e-e+} of pairs produced in the cascade for the tilt angle Θ is presented in Fig. 5. One can see that it essentially grows when Θ approaches π/2. For such tilt angles the electrons arrive at the region of the central electric field antinode earlier (Fig. 6) and, therefore, spend more time in it, which due to the exponential dependence of the multiplicity of A-type cascade on time [6] leads to the growth of the total number of pairs at $\Theta = \pi/2$.

5. Conclusions

The scheme proposed in Ref. [22] and developed here, in which the QED cascades are initiated by ultrarelativistic particles, allows one to solve the problem of premature expulsion of seed particles from the laser field focus. The 'collapse and revival' dynamics of cascades looks much simpler in the case of a small angle of the electron beam tilt with respect to the laser pulses optical axis. However, for increasing the multiplicity of the self-sustained cascade the preferable geometry is $\Theta = \pi/2$.

In the present work, we described the electron beam by an ensemble of particles with similar initial parameters. For conclusions that are more realistic one should take into account that the beam of electrons has finite duration, width and energy spread. However, this does not qualitatively affect the main result of the paper.

Acknowledgements. In the numerical simulations, we used the resources of the NRNU MEPhI high-performace computing centre. The work was supported by the Russian Foundation for Basic Research (Grant Nos 16-02-00963a and 16-32-00863mol_a) and partially supported by the Dynasty foundation.

Appendix. Testing the programme for numerical simulation of cascades using the Monte Carlo method

To check the developed programme we performed a number of tests. In the first test we simulated the cascades initiated by fast electrons with the energy $\varepsilon_0 = 2\times10^5 mc^2$ in the transverse constant uniform magnetic field with the strength $H = 0.2E_s$. The results of the simulations were compared with the cascade profile (the time dependence of the number of the electrons whose energies exceed $10^{-3}\varepsilon_0$), presented in Ref. [29] (Fig. 7). In Ref. [6] we introduced the characteristic radiation time $\tau_{rad} = 3.85(\gamma_{in}/\alpha\chi_{in}^{2/3})(\hbar/mc^2)$, where γ_{in} and χ_{in} is the

Lorentz factor and the dynamic quantum parameter of the initial electron, respectively. As seen from Fig. 7, the results of simulations correspond to the previously published data.

In the second test, we simulated self-sustained cascades in the rotating uniform electric field. The comparison of the calculated dependence of the mean value of the parameter χ and the mean energy of the charged particles on the dimensionless field strength $\mu = E/\alpha E_s$ with the data of Ref. [6] is presented in Fig. 8. We see that the results of the simulations agree with those of Ref. [6] with the error not exceeding 15%. The difference of results can be explained by the fact that, in contrast to Ref. [6], in our programme the recoil effect is completely taken into account in the emission of 'soft' photons with the energy $\varepsilon_\gamma < mc^2$, unable to create a pair of particles.

References

1. Bell A.R., Kirk J.G. *Phys. Rev. Lett.*, **101**, 200403 (2008).
2. Kirk J.G., Bell A.R., Arka I. *Plasma Phys. Control. Fusion*, **51**, 085008 (2009).
3. Fedotov A.M., Narozhny N.B., Mourou G., Korn G. *Phys. Rev. Lett.*, **105**, 080402 (2010).
4. Mourou G., Korn G., Sandner W., Collier J.K. (Eds) *ELI – Extreme Light Infrastructure Science and Technology with Ultra-Intense Lasers. Whitebook* (Berlin: THOSS Media GmbH, 2011).
5. http://www.xcels.iapras.ru/
6. Elkina N.V., Fedotov A.M., Kostyukov I.Yu., Legkov M.V., Narozhny N.B., Nerush E.N., Ruhl H. *Phys. Rev. Spec. Top. Accel Beams*, **14**, 054401 (2011).
7. Duclous R., Kirk J.G., Bell A.R. *Plasma Phys. Control. Fusion*, **53**, 015009 (2011).
8. Nerush E.N., Kostyukov I.Yu., Fedotov A.M., Narozhny N.B., Elkina N.V., Ruhl H. *Phys. Rev. Lett.*, **106**, 035001 (2011).
9. King B., Elkina N., Ruhl H. *Phys. Rev. A*, **87**, 042117 (2013).
10. Ridgers C.P., Brady C.S., Duclous R., Kirk J.G., Bennett K., Arber T.D., Robinson A.P.L., Bell A.R. *Phys. Rev. Lett.*, **108**, 165006 (2012).
11. Kirk J., Bell A., Ridgers C. *Plasma Phys. Control. Fusion*, **55**, 095016 (2013).
12. Di Piazza A., Müller C., Hatsagortsyan K.Z., Keitel C.H. *Rev. Mod. Phys.*, **84**, 1177 (2012).
13. Narozhny N.B., Fedotov A.M. *Eur. Phys. J. Spec. Top.*, **223**, 1083 (2014).
14. Yanovsky V., Chvykov V., Kalinchenko G., et al. *Opt. Express*, **16**, 2109 (2008).
15. Gelfer E.G., Mironov A.A., Fedotov A.M., Bashmakov V.F., Nerush E.N., Kostyukov I.Yu., Narozhny N.B. *Phys. Rev. A*, **92**, 022113 (2015).
16. Bashmakov V.F., Nerush E.N., Kostyukov I.Yu., Fedotov A.M., Narozhny N.B. *Phys. Plasmas*, **21**, 013105 (2014).
17. Grismayer T., Vranic M., Martins J.L., Fonseca R.A., Silva L.O. arXiv:1511.07503 (2015).
18. Jirka M., Klimo O., Bulanov S., Esirkepov T.Z., Gelfer E., Bulanov S., Weber S., Korn G. arXiv:1511.04982 (2015).
19. Bula C. et al. *Phys. Rev. Lett.*, **76**, 3116 (1996); Burke D.L., et al. *Phys. Rev. Lett.*, **79**, 1626 (1997); Bamber C. et al. *Phys. Rev. D*, **60**, 092004 (1999).
20. Bulanov S.S., Schroeder C.B., Esarey E., Leemans W.P. *Phys. Rev. A*, **87**, 062110 (2013).
21. Sokolov I.V., Naumova N.M., Nees J.A., Mourou G.A. *Phys. Rev. Lett.*, **105**, 195005 (2010).
22. Mironov A.A., Narozhny N.B., Fedotov A.M. *Phys. Lett. A*, **378**, 3254 (2014).
23. Fedotov A.M., Elkina N.V., Gelfer E.G., Narozhny N.B., Ruhl H. *Phys. Rev. A*, **90**, 053847 (2014).
24. Nikishov A.I., Ritus V.I. *Zh. Eksp. Teor. Fiz.*, **46**, 776 (1964) [*JETP*, **19** (2), 529 (1964)]; Nikishov A.I., Ritus V.I. *Zh. Eksp. Teor. Fiz.*, **52**, 1707 (1967) [*JETP*, **25** (6), 1135 (1967)].
25. Baier V.N., Katkov V.M. *Phys. Lett. A*, **25**, 492 (1967).
26. Berestetskii V.B., Lifshitz E.M., Pitaevskii L.P. *Quantum Electrodynamics* (Amsterdam: Butterworth-Heinemann, 1982).
27. Agostinelli S. et al. *Nucl. Instr. Meth. A*, **506**, 250 (2003).
28. Vay J.-L. *Phys. Plasmas*,**15**, 056701 (2008).
29. Anguelov V., Vankov H. *J. Phys. G*, **25**, 1755 (1999).
30. Narozhny N.B., Fofanov M.S. *Zh. Eksp. Teor. Fiz.*, **117**, 867 (2000) [*JETP*, **90**, 753 (2000)].
31. Gonoskov A., Bashinov A., Gonoskov I., Harvey C., Ilderton A., Kim A., Marklund M., Mourou G., Sergeev A. *Phys. Rev. Lett.*, **113**, 014801 (2014).